

Break of symmetry in regenerating tobacco protoplasts is independent of nuclear positioning

Linda Brochhausen*, Jan Maisch and Peter Nick

Molecular Cell Biology, Botanical Institute, Karlsruhe Institute of Technology, Kaiserstr. 2, D-76133 Karlsruhe, Germany. *Correspondence: Linda.Aimee@Brochhausen.com

Abstract Nuclear migration and positioning are crucial for the morphogenesis of plant cells. We addressed the potential role of nuclear positioning for polarity induction using an experimental system based on regenerating protoplasts, where the induction of a cell axis *de novo* can be followed by quantification of specific regeneration stages. Using overexpression of fluorescently tagged extranuclear (perinuclear actin basket, kinesins with a calponin homology domain (KCH)) as well as intranuclear (histone H2B) factors of nuclear positioning and time-lapse series of the early stages of regeneration, we found that nuclear position is no prerequisite for polarity formation. However, polarity formation and nuclear migration were both modulated in the transgenic lines, indicating that both phenomena depend on factors

affecting cytoskeletal tensegrity and chromatin structure. We integrated these findings into a model where retrograde signals are required for polarity induction. These signals travel via the cytoskeleton from the nucleus toward targets at the plasma membrane.

Keywords: Axis formation; cytoskeleton; nuclear migration; polarity induction; tobacco BY-2 protoplast

Citation: Brochhausen L, Maisch J, Nick P (2016) Break of symmetry in regenerating tobacco protoplasts is independent of nuclear positioning. *J Integr Plant Biol* 58: 799–812 doi: 10.1111/jipb.12469

Edited by: Haiyun Ren, Beijing Normal University, China

Received Jan. 5, 2016; **Accepted** Feb. 16, 2016

Available online on Feb. 22, 2016 at www.wileyonlinelibrary.com/journal/jipb

© 2016 Institute of Botany, Chinese Academy of Sciences

INTRODUCTION

How cells acquire polarity and axis remains a central question of plant morphogenesis. While polarity in animals is usually systemic in nature and is generated through the interaction of different cell types, plant polarity seems to be rooted directly within the individual cell (Vöchting 1878). Axis and polarity are mostly inherited from the maternal cell (Nick 2011), raising the question of how polarity and axis are established *de novo*. A classic system for polarity induction has been the *Fucus* zygote (Goodner and Quatrano 1993; Hable and Hart 2010). Similar cases of symmetrical, freely accessible cells, which undergo formative divisions, are rare in higher plants. As an alternative to studying polarity induction *de novo*, polarity can be artificially eliminated by digesting the cell wall with cellulases. This *tabula rasa* approach yields protoplasts, which, in most cases, are round and apparently have lost axis and polarity. Nevertheless, they can be induced to regenerate complete plants, as has been demonstrated for the first time for tobacco (Nagata and Takebe 1970). Upon standardization of the system, Zaban et al. (2013) were able to generate quantitative data on the temporal patterns of regeneration due to classification into distinct stages. The synthesis of a new cell wall marks the transition to the first important stage of regeneration and proceeds, after a long preparatory phase, within a few minutes. During this preparatory phase, the nucleus actively migrates. This indicates that nuclear migration is linked with the induction of polarity in axis.

Nuclear migration has been described in great detail for many different organisms such as *Drosophila melanogaster*, *Saccharomyces cerevisiae*, *Aspergillus nidulans*, and *Caenorhabditis elegans* (for review see Morris 2000, 2003). The

molecular components responsible for positioning and movement of the nucleus are moderately conserved among these well-characterized model organisms and comprise dynein, dynactin, as well as other microtubule and actin linker proteins.

Also in plants, nuclear migration plays a pivotal role for a wide range of several cellular processes. These include development of pollen tubes, trichomes and root hairs, symbiotic and pathogenic plant–microbe interactions, responses to mechanical and blue light stimuli, and symmetric, as well as asymmetric cell divisions (for review see Griffis et al. 2014). As characterized for stomatal development, pre-mitotic nuclear migration is linked to the position of asymmetric division planes which are oriented with respect to the polarity of the mother cells (for review see Smith 2001). There exist several examples that demonstrate the importance of nuclear positioning for symmetry and plane of the ensuing cell division, although the mechanistic link between nuclear migration and the induction of cell axiality is far from understood.

In the experimental protoplast regeneration model already mentioned (Zaban et al. 2013), the re-establishment of a cell wall is heralded by a phase of vivid nuclear motility, where the nucleus is searching for a central position, similar to the situation when a vacuolated cell prepares for cell division. Here, the position of the nucleus determines the division plane while cytoplasmic strands rearrange in a pattern predicting the site of the prospective cell plate (for review see Nick 2008). Both cytoskeletal elements, actin filaments as well as microtubules, participate in nuclear migration and tethering (Katsuta and Shibaoka 1988). Unlike nuclear positioning in fungi and insects, plants lack dynein and thus

a dynactin complex, and therefore must employ other proteins for the dynamic cross-link of actin and microtubules in pre-mitotic nuclear migration.

In fact, a plant subgroup of the kinesin-14 family, the KCH kinesins (for “kinesins containing a calponin-homology domain”) were identified as microtubule-actin filament cross-linkers (for recent review see [Schneider and Persson 2015](#)). As these motor proteins are capable of minus-end directed movement, the KCHs might be the functional homologues of dyneins. In addition to the characteristic microtubule-binding kinesin motor domain, KCH-proteins possess a conserved calponin-homology (CH) domain, well known as actin binding motif from a variety of actin-associated proteins such as α -actinin, spectrin and fimbrin. Thus, KCHs mediate between both cytoskeletal elements and bind to both elements of the cytoskeleton. Both the rice member OsKCH as well as the tobacco member NtKCH have been shown to modulate premitotic nuclear positioning in tobacco BY-2 ([Frey et al. 2010](#); [Klotz and Nick 2012](#)). To understand the role of nuclear migration in cell polarity, two factors of KCH play an important role: KCH exists in two functionally different subpopulations, either uncoupled from actin in a mobile form that moves along microtubules of the interphase cortex and the phragmoplast, or coupled to actin in a static form in the premitotic radial array of cytoplasmic microtubules ([Klotz and Nick 2012](#)). This actin-bound form of KCH accumulates also on the nuclear envelope prior to the onset of mitosis, suggesting a role of actin-linked KCH for nuclear positioning.

In animal cells, the nuclear envelope is structured by a subtending nuclear lamina, which is highly important for nuclear positioning and movement. Several proteins link the lamins to the cytoskeleton ([Malone et al. 1999](#); [Lee et al. 2002](#)). However, nuclear lamins have remained elusive in plant cells so far. Instead, a perinuclear actin basket has been reported ([Wang and Nick 1998](#)). Recently, this perinuclear actin basket could be specifically visualized by a tetrameric Lifeact fused to a photoswitchable red fluorescent protein (Lifeact-psRFP). The yeast peptide Lifeact is well known to bind to a ubiquitous motif in F-actin. In [Durst et al. \(2014\)](#) it was fused to a tetrameric photoswitchable red fluorescent protein (psRFP, [Fuchs 2011](#)). Due to its large size, this fusion construct should be sterically prevented from binding to actin via the Lifeact motif, when the actin filament is densely decorated with actin-binding proteins, whereas the construct should readily bind to uncovered actin. Using this marker, z-stacks of the actin basket could be collected by photoactivated localization microscopy (PALM) in a resolution of 20 nm ([Durst et al. 2014](#)). Super-resolution microscopy showed that the perinuclear actin cage was wrapped around the nuclear envelope in a lamellar fashion.

The structure of the chromatin should influence nuclear migration as well. In fact, epigenetic changes in histone packaging can result in changes of nuclear architecture ([Bartova et al. 2008](#)). Overexpression of core histones such as in the line histone H2B monomeric Eos fluorescent protein (H2B-mEos) ([Wozny et al. 2012](#)) might be used to test this supposition, which to our knowledge has not been addressed experimentally, so far.

The intensive nuclear movements observed during the first day of protoplast regeneration ([Zaban et al. 2013](#)) indicate

a link between nuclear positioning and the formation of axis and polarity. In the current work, we want to test the hypothesis, whether nuclear positioning is a prerequisite for the re-establishment of axis and polarity. To address this, we manipulated the nuclear migration on a genetic level by overexpression of fluorescently tagged players of nuclear movement (Lifeact-psRFP, green fluorescent protein (GFP)-NtKCH, H2B-mEos). By overexpression of these components, we tried to modulate both extranuclear (perinuclear actin basket, KCH) as well as intranuclear (histone H2B) factors supposed to act on nuclear movement. The effect of these manipulations on nuclear migration was followed via time-lapse movies and could then be compared with respect to their impact on axis and polarity by quantitative analysis of the regeneration pattern. We found that induction and manifestation of cell axis can be uncoupled from nuclear positioning, but that both phenomena depend on factors that affect cytoskeletal tensegrity (perinuclear actin basket, KCH), as well as on factors acting on chromatin structure. We integrated these findings into a model, where cytoskeletal tensegrity acts as a common factor for both nuclear positioning and the formation of axis and polarity.

RESULTS

Classification of different regeneration stages

In order to follow the formation of polarity and axis *de novo*, a staging system modified from [Zaban et al. \(2013\)](#) was used to generate quantitative data on the temporal patterns of regeneration ([Figure 1](#)). Since the formation of a cell axis is preceded by the formation of a new polarity ([Zaban et al. 2013](#)), in the following, for pragmatic reasons, we will mainly use the term axis formation (implying that polarity induction has been successfully completed, when cell axis becomes visible).

Based on clearly delineated differences in cell shape and cell-wall reformation, the cells could be clearly assigned to one of five stages schematically represented in [Figure 1](#). Stage 1, prevailing at the end of digestion (defined as $t = 0$), comprised round, completely symmetrical protoplasts lacking any indications for axis or polarity. The nucleus is mostly ovoid in shape and placed at the periphery. Subsequently, the nucleus moves from the periphery of the cell toward the cell center and becomes spherical. About 12–24 h later, a new cell wall has been first synthesized as visualized by staining with Calcofluor White. These cells still show radial symmetry and are classified into stage 2. Between d 1 and d 2 of regeneration, cell shape changes distinctly, and a clear cell axis emerges leading to an ovoid shape. The presence of a cell axis represents the criterion for stage 3. Subsequently, this axis becomes manifest as cell elongation. Cells, where the long axis has reached a length, which is more than twice as long as the short axis, fall into stage 4. At this stage, some of the cells already begin to divide axially, producing the pluricellular files characteristic of tobacco suspension cells. These files are indistinguishable from those derived from walled cells. During this final step of regeneration, the nucleus is still tethered at the cell center and has become elliptic, whereby its longer axis is parallel to the elongation axis. Failure in axis manifestation leads to cells where a third pole emerges.

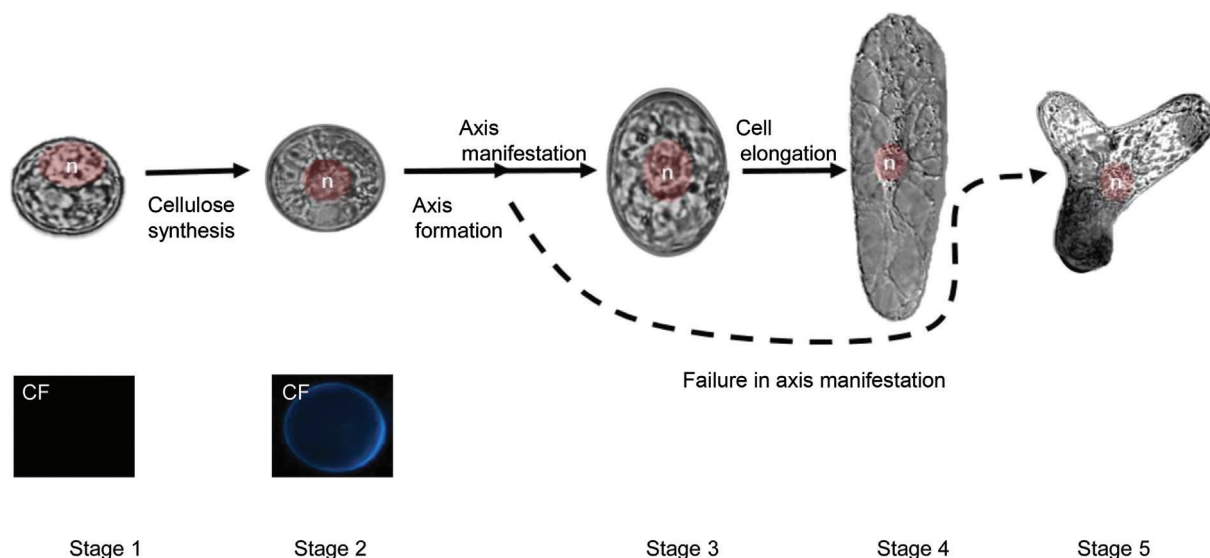


Figure 1. Classification of different regeneration stages

Classification into distinct stages (according to [Zaban et al. 2013](#)) used for the current study to follow nuclear position (highlighted in red) in the context of axis formation. Stage 1 is defined by the absence of the cell wall. The protoplasts are completely spherical, the nucleus (n) is mostly located at the periphery. Stage 2 is defined by the presence of the cell wall which can be visualized by staining with Calcofluor White (CF, scale bars = 20 μm). Cells are still symmetrical. Stage 3 is defined by a break of radial symmetry. A clear axis emerges and axis becomes manifest. Stage 4 is defined by the elongated cell axis. Stage 5 occurs if axis manifestation is disturbed (dashed line) and tripolar structures are generated.

These aberrant tripolar cells are defined as stage 5. In these cells, the position of the nucleus does not follow any obvious rule.

The relative frequencies of these five different stages were scored over time. In order to understand the role of nuclear positioning for axis formation, in addition to the non-transformed BY-2 cell line, three different transgenic cell lines were used, including a perinuclear actin marker line (Lifeact-psRFP), a class XIV-kinesin overexpression line (GFP-NtKCH) and a histone marker line (H2B-mEos). In these lines, the nuclear positioning from the cell periphery to the cell interior was altered. This allowed probing for potential changes of regeneration patterns in consequence of altered nuclear positioning. In the following, first the effect of the overexpressions on the regeneration patterns will be described, whereas in the final part of the result section, the effect upon nuclear migration will be compared.

Overexpression of the perinuclear actin marker Lifeact-psRFP promotes axis formation, but perturbs axis manifestation

Since the perinuclear actin cage is important for nuclear movement, we used the transgenic line Lifeact-psRFP, in which only the actin filaments of this perinuclear cage are labelled via a photoswitchable RFP. The temporal pattern of regeneration in the Lifeact-psRFP line was compared to the situation in the non-transformed BY-2 wild-type cell line ([Figure 2](#)).

Already after the first day of regeneration, the majority of the transgenic cells had formed a new cell wall, thus entering stage 2. Only some 10% were still lacking a cell wall, which was in sharp contrast to non-transformed cells, where around 60%

of the cells still had not generated a cell wall. A significant fraction (30%) of the Lifeact-psRFP cells had even already passed the transition to stage 3, which is defined by an ovoid cell shape, compared to only 5% in the non-transformed cell line. Even at day 2 of regeneration, the transgenic lines remained ahead with more than 40% of the cells in stage 3 in comparison to about 25% in the non-transformed cell line. At this time point, first deviations from the normal sequence of events became detectable: more than 40% of the Lifeact-psRFP cells started to divide prematurely (in stage 3), although axis manifestation had not yet initiated, which was different from the non-transformed control (see [Figure S1](#)). Also, in many cells, during day 3 after regeneration, a second competing axis was observed, leading to a significantly higher frequency of tripolar structures (stage 5), compared to the non-transformed cell line. Although the initial course of regeneration was accelerated in the transgenic line, the transition from stage 3 to 4 (axis manifestation, normally at day 4) was not (indicating that the transgenic cells required more time to leave stage 3). From day 5, the frequency distributions of the transgenic line were not distinguishable from those of the non-transformed controls, indicating that the transition from stage 3 to 4 was not arrested, but just delayed by overexpression of the transgene. Thus, axis formation was significantly promoted by the Lifeact-psRFP cell line, whereas the final step of regeneration, axis manifestation, was delayed, correlated with a higher frequency of aberrant tripolar structures in the transgenic line compared to the non-transformed cell line. To test whether these deviations are a consequence of overexpression *per se*, we employed a cell line where free GFP was overexpressed under the same promoter (CaMV-35S). The

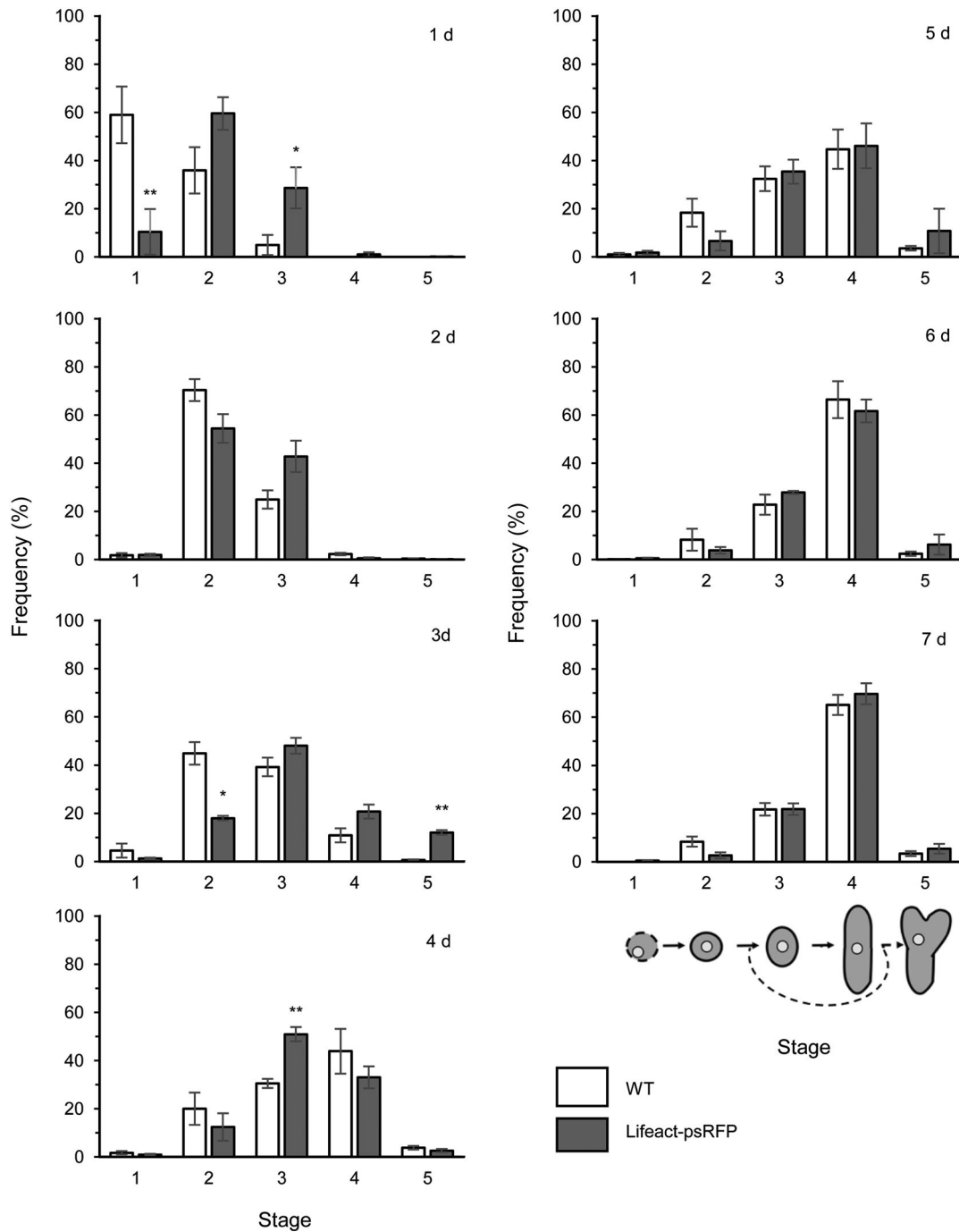


Figure 2. Frequency distributions of regenerations stages in BY-2 Lifact-psRFP

Frequency distributions of the different regeneration stages for different time points after protoplast preparation in BY-2 Lifact-psRFP (grey bars) compared to non-transformed BY-2 (white bars). Stages are indicated schematically. Frequency distributions have been calculated from 3,000 individual cells per time point from three independent biological replications. Error bars show standard errors of the mean (SE). Asterisks represent significance of indicated differences as tested by a paired, two-side t-test (*P < 5%, **P < 1%). WT, wild type; Lifact-psRFP, Lifact fused to a photoswitchable red fluorescent protein.

regeneration pattern of this 35S::GFP line was exactly the same as that of non-transformed controls (see Figure S2) suggesting that the effects observed in the Lifact-psRFP line were specific to the overexpression of the perinuclear actin marker.

Overexpression of the class XIV kinesin KCH promotes both axis formation as well as axis manifestation

Motor proteins, which run along the cytoskeleton, play a pivotal role for organelle movement. Since microtubules, as well as actin filaments, participate in nuclear positioning, the

class-XIV kinesin NtKCH as cross-linker of these cytoskeletal elements is interesting. Therefore, regeneration in a GFP-NtKCH overexpressor line was compared to the regeneration of non-transformed wild-type cells (Figure 3).

Similar to the Lifeact-psRFP cell line, the early phases of regeneration were promoted in the GFP-NtKCH overexpression line. At day 1, less than 10% of the transgenic cells were in stage 1 in comparison to about 60% in non-transformed cells. GFP-NtKCH cells in stage 3 were already predominant after 1 d, which means that most of the cells had built an axis by this time. Around 10% had even developed further to stage 4, which was not the case for non-transformed cells. During d 2 and 3 after regeneration, the frequency of cells in stage 4 increased rapidly in the GFP-NtKCH line compared to the non-transformed line. At day 3, already 60% of the cells were elongated, that is they had expressed their axis, whereas only 10% of the non-transformed cells had reached this stage 4. At d 4 and 5, the kinesin overexpression line showed a higher frequency of cells in stage 4 compared to non-transformed cells. At d 6 and 7, the regeneration pattern of the transgenic line and the non-transformed line had approximated. In contrast to the Lifeact-psRFP, no tripolar cells were observed during regeneration of GFP-NtKCH. Overall, the regeneration was clearly faster in the GFP-NtKCH overexpression line, which can be attributed to an accelerated axis formation. Whereas axis manifestation was delayed upon overexpression of Lifeact-psRFP, the overexpression of GFP-NtKCH did not impair axis manifestation, which is evident from the efficient progression into stage 4 and the absence of aberrant tripolar structures. It should be mentioned that we also tested overexpression of OsKCH, a heterologous KCH from rice. The effect of GFP-OsKCH was comparable to that of GFP-NtKCH, but the amplitude of the effect was less pronounced (see Figure S3). Additionally, we tested the effect of eliminating microtubules via Oryzalin treatment. Compared to the untreated wild-type cells, polarity induction as well as axis formation were clearly delayed and axis elongation (stage 4) hardly occurred until d 7 (see Figure S4).

Overexpression of the histone marker H2B-mEos promotes axis formation, but delays axial cell expansion

Since plants lack a canonical nuclear lamina, nuclear migration is expected to depend not only on extranuclear factors or the activity of motor proteins, but also on the intranuclear architecture. Hence, we tested a cell line in which a labelled histone (H2B-mEos) was overexpressed to probe for potential effects of intranuclear architecture on the regeneration pattern (Figure 4).

Similar to the other transgenic lines, the early progression of regeneration was also promoted in the H2B-mEos line, from only 1 d after regeneration; the majority of protoplasts had reached stages 2 and 3. Moreover, at the same time, already around 40% of the cells had advanced to stage 3 in comparison to only about 5% in the non-transformed cell line. Although the frequency of stage 3 rose even further during the second day, this was not followed by an increased frequency of stage 4: While at d 3, the frequency of stage 3 cells had increased to 60%, only 5% of cells were found to have reached stage 4, which was even less than the value for non-transformed cells (10%), that derived from a significantly lower level of stage 3

precursors. Thus, H2B-mEos cells remained temporarily trapped in stage 3, maintaining an ovoid cell shape with a delay of elongation growth. Although significantly delayed, this elongation ensued eventually: The frequency distributions for d 5, 6 and 7 progressively approached those of the non-transformed cell line, only with a somewhat smaller frequency of transformed cells at stage 4 compared to non-transformed cells. However, despite the delay in cell expansion, barely any tripolar structures were observed, not in the H2B-mEos or in the non-transformed line. Overall, in H2B-mEos, axis formation at the early phases of regeneration was promoted, and the initial steps of axis manifestation proceeded normally. However, the strong cell elongation driving the transition of stage 3 to stage 4 was delayed.

Nuclear positioning can be separated from axis formation

In order to investigate the question whether nuclear positioning is required for the formation of axis and polarity, time-lapse studies were conducted (Figure 5). From the previous data, it was evident that the early stages of regeneration were the most significant, since already after 1 d the regeneration patterns in the three transgenic lines clearly differed from the situation in the non-transformed line. We therefore followed the initial phase of nuclear migration and polarity formation during the first day in individual cells. These differences became detectable from around 9 h after regeneration, which was therefore scrutinized as a critical time point. Representative images from these time-lapse series of the three transgenic lines compared to the non-transformed line are shown in Figure 5 and the movies are given in the supplementary material.

At the onset of regeneration ($t = 0$ h), the nucleus of the non-transformed cell line was elliptical in shape and located at the periphery (Figure 5A, white arrow). It should be noted that protoplasts were generated at the peak of the proliferation phase, 3 d after subcultivation, which means that prior to cell-wall digestion, most nuclei were in the cell center (Figure S4). After 9 h of regeneration, the nucleus began to round up and to shift slowly from the cell wall to the cell center (Figure 5B, white arrow). The cell was still round with no indications of changes in size or shape at this stage. After 1 d, the nucleus had reached the cell center and the cell expanded symmetrically (Figure 5C, dashed yellow arrows), but no indications of cell axis or polarity were detectable.

To test for a potential influence of the perinuclear actin basket on nuclear migration and the formation of axis and polarity, we analyzed Lifeact-psRFP cells. Here, the nucleus was already tethered at the cell center $t = 0$ h, that is straight at the end of cell-wall digestion, and it was not elliptical, but round (Figure 5D, white arrow). At 9 h, axis formation had already started (Figure 5E, dashed yellow arrow), and the nucleus was still positioned in a central position (Figure 5E, white arrow). At 24 h, the cells were clearly ovoid, that is axis manifestation had continued (Figure 5F). The nucleus, still positioned at the cell center, had become enlarged after 24 h (Figure 5F, white arrow).

Since the nucleus is moved via interaction of actin filaments and microtubules, a cell line which overexpresses the class-XIV kinesin KCH was investigated. Similar to the non-transformed line, in GFP-NtKCH the nucleus was positioned at

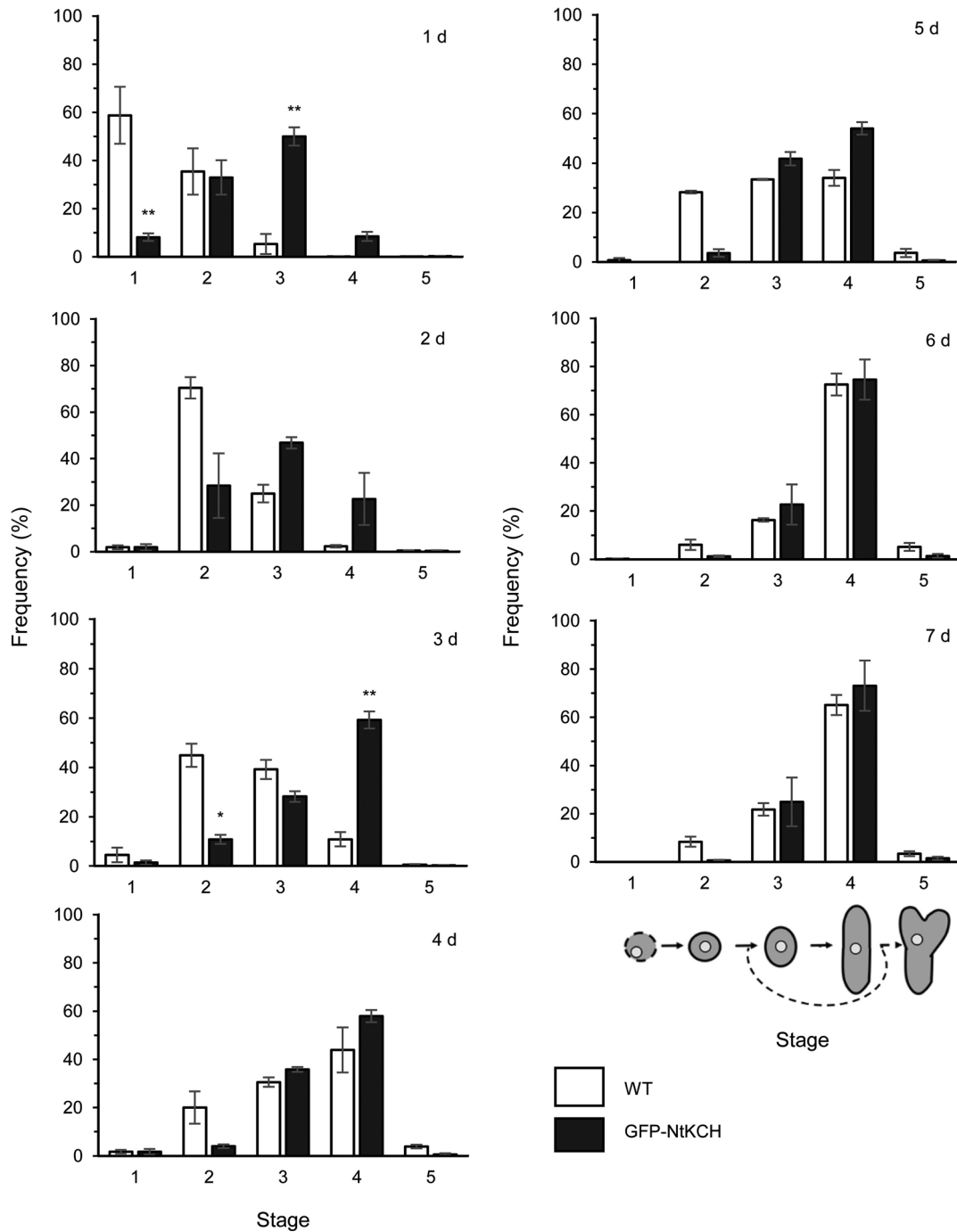


Figure 3. Frequency distributions of regenerations stages in BY-2 GFP-NtKCH

Frequency distributions of the different regeneration stages for different time points after protoplast preparation in BY-2 GFP-NtKCH (dark grey bars) compared to non-transformed BY-2 protoplasts (white bars). Stages are indicated schematically. Frequency distributions have been calculated from 3,000 individual cells per time point from three independent biological replications. Error bars show standard errors of the mean (SE). Asterisks represent significance of indicated differences as tested by a paired, two-side t-test (* $P < 5\%$, ** $P < 1\%$). WT, wild type; GFP-NtKCH, green fluorescent protein tobacco member kinesins with a calponin homology domain.

the periphery at the onset of regeneration, and the protoplast was round (Figure 5G, white arrow). At 9 h, axis formation had already initiated (Figure 5H, dashed yellow arrow). However, the nucleus was moving slower than in the non-transformed

cell line and hence was still located at the periphery (Figure 5H, white arrow). Only at 24 h had the nucleus eventually reached the cell center, while axis formation had already proceeded further (Figure 5I, white arrow).

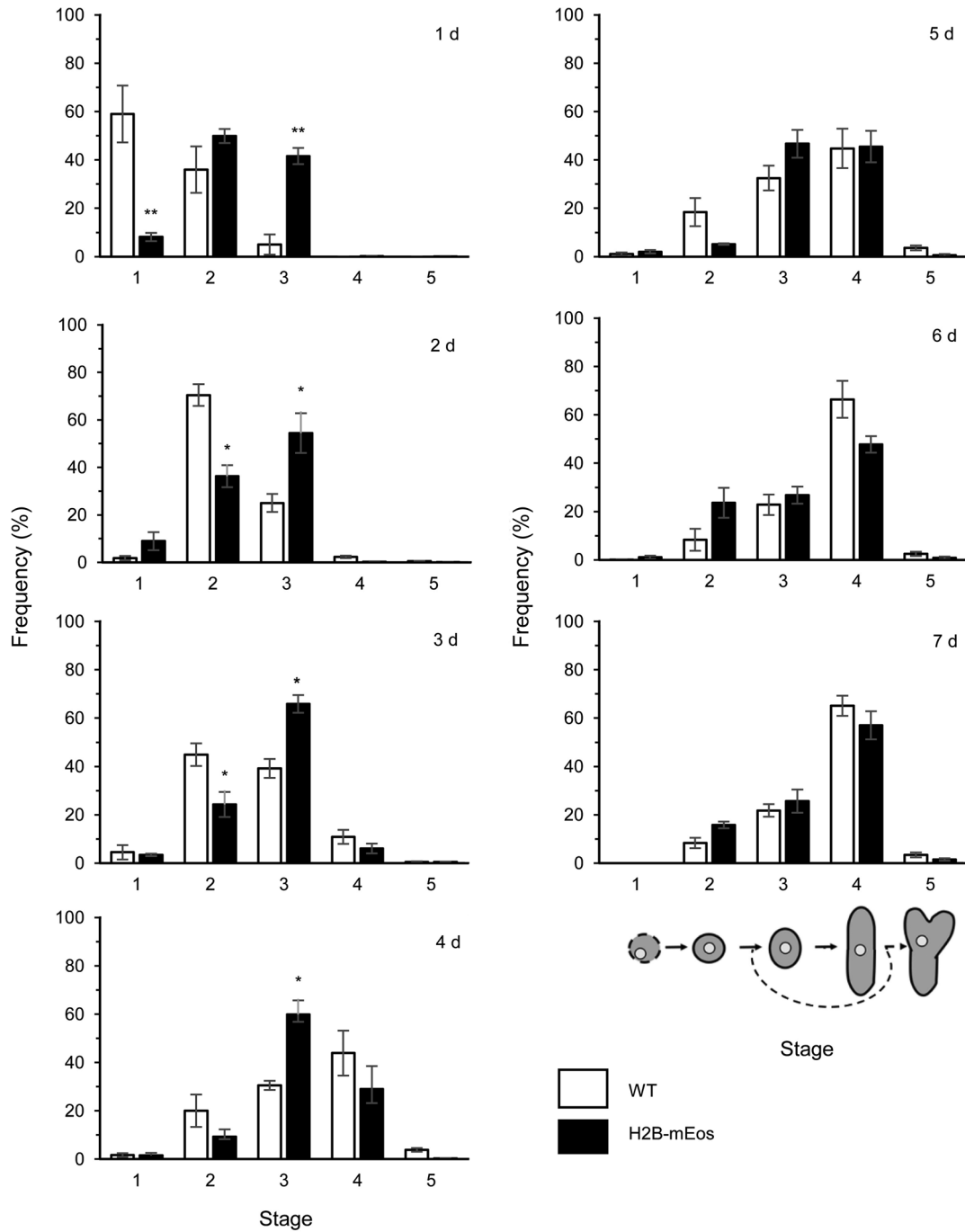


Figure 4. Frequency distributions of regenerations stages in BY-2 H2B-mEos

Frequency distributions of the different regeneration stages for different time points after protoplast preparation in BY-2 H2B-mEos (black bars) compared to non-transformed BY-2 protoplasts (white bars). Stages are indicated schematically. Frequency distributions have been calculated from 3,000 individual cells per time point from three independent biological replications. Error bars show standard errors of the mean (SE). Asterisks represent significance of indicated differences as tested by a paired, two-side t-test (* $P < 5\%$, ** $P < 1\%$). WT, wild type; H2B-mEos, histone H2B monomeric Eos fluorescent protein.

To probe for potential alterations of chromatin structure, the H2B-mEos cell line was investigated. Since axis formation was promoted in this cell line, we were interested to see nuclear migration during the first day of regeneration. At the end of cell-wall digestion ($t = 0$ h), the nucleus was located at

the periphery, similar to the situation in the non-transformed control (Figure 5J, white arrow). At 9 h, the cell already started to elongate (Figure 5K, dashed yellow arrow), although the nucleus was still at the periphery. Interestingly, the nucleus was partially separated into two interconnected lobes

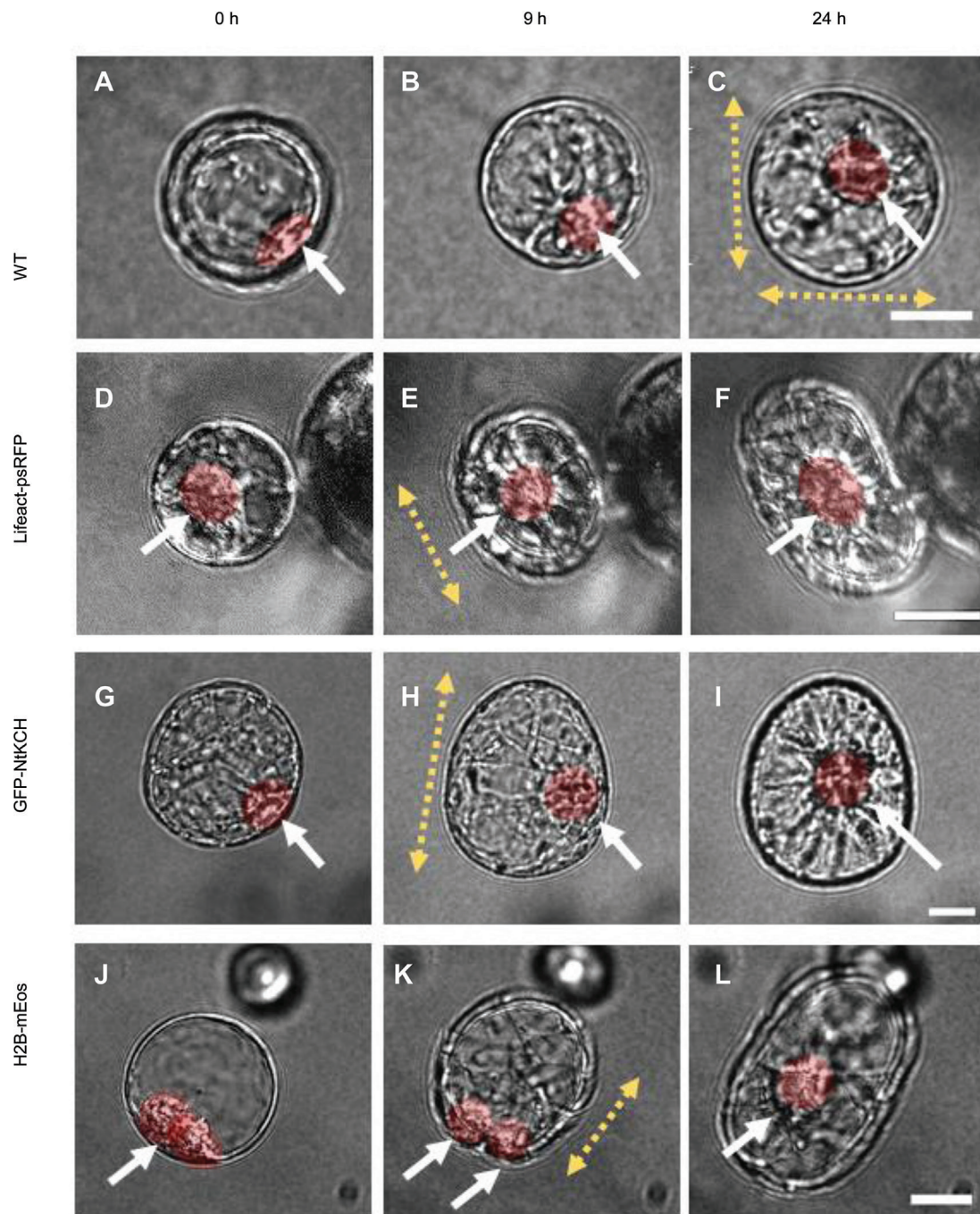


Figure 5. Time-lapse series after protoplast generation

Representative images from time-lapse series recorded from individual cells at 0 h (A, D, G, J), 9 h (B, E, H, K) and 24 h (C, F, I, L) after generation of protoplasts, respectively, for non-transformed BY-2 WT (A, B, C), Lifact-psRFP (D, E, F), GFP-NtKCH (G, H, I), and H2B-mEos (J, K, L). The nucleus is shadowed in red, and indicated by white arrows. Yellow arrows indicate the orientation of the ensuing axis formation. Scale bars = 20 μ m. WT, wild type; Lifact-psRFP, Lifact fused to a photoswitchable red fluorescent protein; GFP-NtKCH, green fluorescent protein tobacco member kinesins with a calponin homology domain; H2B-mEos, histone H2B monomeric Eos fluorescent protein.

(Figure 5K, white arrows). At 24 h, these two lobes had again merged into one complete nucleus which slowly moved into the cell center (Figure 5L, white arrow). At this time, axis manifestation had already started.

DISCUSSION

Since nuclear movement is important for several processes in plant cells, we wanted to know which role nuclear movement

plays in polarity and axis formation, and to test whether a central nuclear positioning is a prerequisite for polarity and axis induction. By means of analyzing regeneration of protoplasts, it is possible to follow the induction and manifestation of a cell axis *de novo*. In order to manipulate the nuclear movement on a genetic level, we used three different cell lines overexpressing key players involved in nuclear positioning: In the Lifeact-psRFP cell line a specific actin basket around the nucleus was labelled; in the GFP-NtKCH cell line, a motor protein acting as a cross linker of actin and microtubules is overexpressed; and in the H2B-mEos cell line, a histone is overexpressed and expected to affect intranuclear architecture. By quantification of specific regeneration stages, the temporal patterns of these overexpression lines could be compared to the non-transformed line. Overexpression of the perinuclear actin marker line promoted axis formation in the beginning, but later perturbed axis manifestation, whereas overexpression of the class XIV kinesin KCH promoted both axis formation and axis manifestation. Overexpression of the histone marker promoted axis formation, but delayed cell elongation. Time-lapse studies of nuclear movement during the early stages of regeneration were used to relate the nuclear positioning and the induction of axis and polarity.

Is a central position of the nucleus a necessary prerequisite for polarization?

Nuclear positioning is necessary for the correct geometry of the subsequent cell division (reviewed in Smith 2001). Hence, we asked whether a central position of the nucleus might also be a prerequisite for polarity induction. Time-lapse studies of the moving nucleus in the early stages of regeneration clearly argue against this hypothesis and demonstrate that nuclear positioning can be separated from axis formation (see Figure 5).

At first sight, when we followed nuclear migration of the Lifeact-psRFP cell line, the presumed link between nuclear position and axis formation appeared to be valid. Here, the nucleus was already tethered at the cell center and axis formation started earlier compared to the non-transformed cell line (Figure 6A, B). However, for the GFP-NtKCH cell line, axis formation initiated earlier than in the non-transformed line, whereas the nucleus was still not located at the cell center (Figure 6A, D). Similarly, in the H2B-mEos line, axis formation had already started, before the nucleus had reached the cell center (Figure 6C). Thus, a central nuclear position is not necessary for axis formation, but rather seems to be a parallel phenomenon.

Nuclear positioning depends on perinuclear actin, KCH and chromatin structure

Although nuclear positioning and cell axis were uncoupled, both phenomena were clearly dependent on the extra- and intranuclear factors addressed by the three transgenic lines.

As plants lack a nuclear lamina meshwork, which is involved in nuclear migration and provides mechanical stability of the nucleus in animal cells (for review see Goldman et al. 2002), there must be structural analogues to the mammalian lamina in plant cells. In fact, a perinuclear cage has been reported (Wang and Nick 1998), and is specifically visualized by the Lifeact-psRFP marker (Durst et al. 2014).

Whereas during protoplast preparation, the G₂ nucleus loses its central position and shifts to the periphery, it remains tethered in the cell center when the protoplasts are prepared from the Lifeact-psRFP line, indicative of a more stable perinuclear basket. Therefore, the perinuclear actin basket behaves as a functional homologue of the nuclear lamina, but also seems to be involved in the migration of the nucleus.

Class XIV kinesins with a calponin homology domain (KCH) have been identified as important factors of premitotic nuclear positioning (Frey et al. 2010; Klotz and Nick 2012). In functional analogy to dyneins that convey this function in animal and fungal cells (reviewed in Morris 2000, 2003), KCH crosslinks actin filaments with microtubules. The mechanically rigid microtubules can confer compression forces and would, together with the flexible actin filaments that can confer traction forces, establish a tensegral system able to sense and integrate mechanic forces between cell periphery and nucleus (reviewed in Nick 2011). As mentioned before KCH can either occur in a free, mobile state (not linked with actin) or in a static situation cross-linked to actin (Klotz and Nick 2012). Both the nuclear migration at the onset of protoplast regeneration (see Figure 5), as well as premitotic nuclear positioning in walled cells (Frey et al. 2010) were clearly delayed.

Not only extranuclear, but also intranuclear factors, were relevant for nuclear positioning. Indeed, we observed that overexpression of a histone caused a delay of nuclear movement. This functional change is accompanied by a clear change of nuclear architecture, resulting in distorted nuclear shape during early regeneration (see Figure 5). This obviously changed nuclear architecture indicates that histones, in addition to their role in transcriptional activity, are important for intranuclear architecture. Although histones are highly conserved, studies showing that specific modifications and variants of histones (Verbsky and Richards 2001; Fransz and de Jong 2002; Yi et al. 2006; Deal and Henikoff 2011) not only contribute to several nuclear functions including DNA repair, transcription, replication, or chromosome condensation (Kouzarides 2007), but also may lead to changed chromatin architectures (Ahmad and Henikoff 2002; Smith et al. 2002; Talbert et al. 2002). As the DNA wraps around the highly conserved core histones forming the nucleosomes, it is to be expected that the overexpression of the H2B-mEos marker, as affecting one of the four core histones, should affect DNA packaging and therefore cause changed intranuclear architecture and flexibility. The resulting higher “viscosity” should then reduce the velocity of the nucleus (Figure 6C).

Polarization depends on perinuclear actin, KCH and chromatin structure

While the effects of perinuclear actin, KCH and chromatin structure on nuclear movement can be understood in terms of activities around (actin, KCH) or inside (chromatin) the nucleus, the effect of these factors on polarization and axis formation has to be located at the plasma membrane. Our results show that manipulation of factors which are involved in the nuclear movement also result in different regeneration patterns. We demonstrated that overexpression of the perinuclear actin marker Lifeact-psRFP promotes axis formation, but perturbs axis manifestation (see Figure 2). This is surprising at first sight: Why should alterations of actin at the nuclear envelope affect actin-related processes occurring

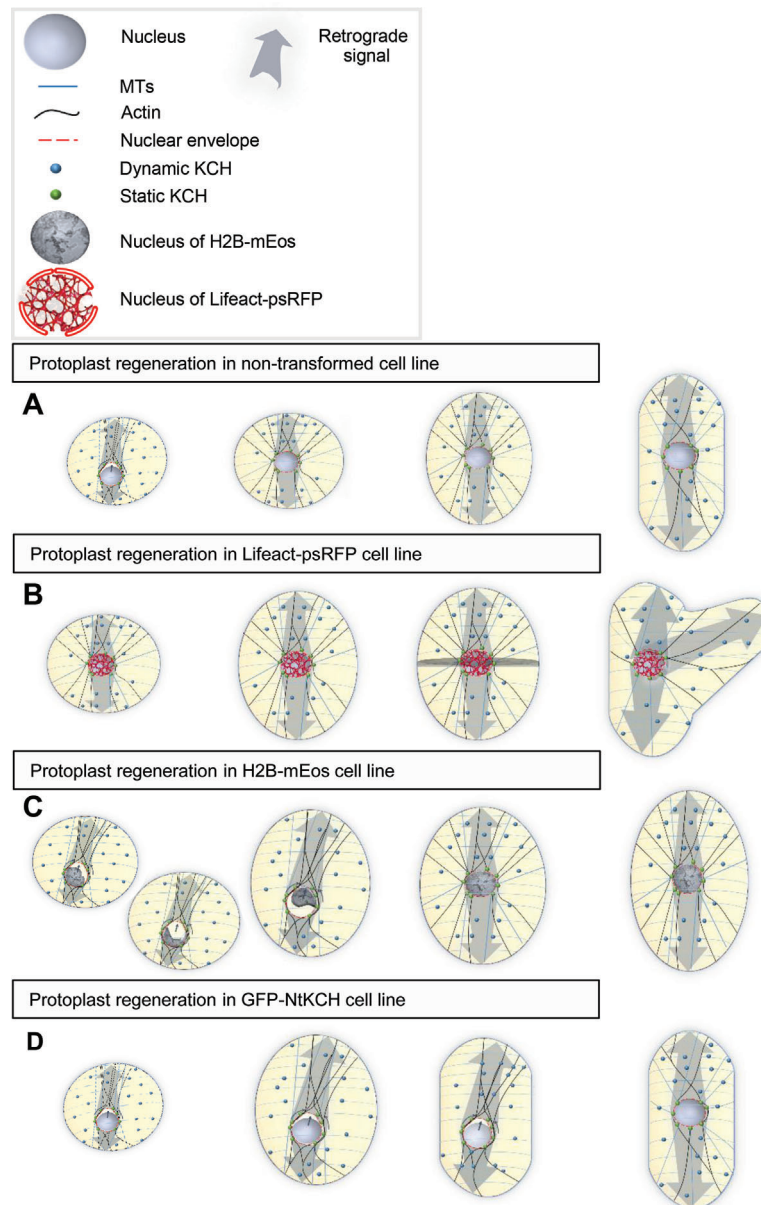


Figure 6. Model of nuclear migration during polarity induction and axis formation

Model of nuclear migration during polarity induction and axis formation from the onset of polarity induction until elongated cells in the non-transformed cell line (**A**), Lifeact-psRFP cell line (**B**), H2B-mEos cell line (**C**), GFP-NtKCH cell line (**D**). With the onset of polarity formation the nucleus starts to migrate into the cell center (black arrow): static KCHs (green spheres) decorate the perinuclear network (red dashed lines) and are connected with radial microtubules (MTs, blue lines); dynamic KCHs are located in the cortex (blue spheres) and move along cortical MTs (blue horizontal lines), generating sliding forces that act on the nucleus (large grey sphere). Retrograde signals are transported from the nucleus through the cytoskeleton (actin-filaments AF, MTs) to targets at the plasma membrane (semi-transparent arrows). After a few hours the nucleus has reached the cell center; the protoplast has expanded circularly, followed by axis formation, axis manifestation and further cell elongation whereby the long axis is more than twice as long as the short axis (**A**). Compared to the non-transformed cell line, the nucleus of the Lifeact-psRFP cell line (red basket) is already located at the cell center from the onset of polarity induction; axis formation is promoted, followed by division of protoplasts at oval stages, resulting in an increase of tripolar structures (**B**). The nucleus of the H2B-mEos cell line shows an abnormal nuclear architecture (grey patterned nucleus) and therefore its shape might slow down the movement, whereby axis formation is started until the nuclear shape is normal again and eventually is located at the cell center; the long cell axis is more than twice as long as the short axis; however, the cells are shorter than the non-transformed cells (**C**). Compared to the non-transformed cell line, axis formation in the GFP-NtKCH cell line is faster and nuclear migration is slowed down at the early phases (**D**). Lifeact-psRFP, Lifeact fused to a photoswitchable red fluorescent protein; GFP-NtKCH, green fluorescent protein tobacco member kinesins with a calponin homology domain; H2B-mEos, histone H2B monomeric Eos fluorescent protein.

underneath the plasma membrane? This retrograde signaling from the perinuclear actin toward the plasma membrane is less surprising in the conceptual framework of a tensegral cytoskeleton. The overexpression of the Lifeact actin marker presumably causes a stabilization of the perinuclear cage or makes it more resistant against reorganization of actin filaments because of additional crosslinks, which through the radial actin cables should alter traction forces acting on the anchoring sites at the plasma membrane. This may underlie the promoted induction of asymmetry observed in the Lifeact-psRFP line. However, to translate this polarity into a new cell axis, actin dynamics is required (Zaban et al. 2013). Thus, reorganization of actin filaments is prerequisite for manifestation of the reformed axis. The Lifeact-psRFP shows a high amount of premature cell division of cells in an oval stage, that is in cells, where axis formation was initiated, but axis manifestation had not yet been completed (Figure 6B). This aborted axis manifestation is responsible for the relatively high incidence of tripolar structures. These tripolar structures derive from perturbations of simple polarities, when a second, competing pole is laid down ectopically. In contrast to a complex polarity, where both poles along an axis are defined by specific molecules or activities, the polarity of plant cells is often simple, that is only one pole is explicitly defined, whereas the opposing pole is simply characterized by the absence of the polarizing molecules or activities (Nick and Furuya 1992).

Axis formation and elongation also require a close interplay of both actin filaments and microtubules. While KCH overexpression delays nuclear migration, cell elongation is stimulated (Figure 6D). Promoted cell elongation at simultaneously retarded nuclear migration has also been found for walled cells overexpressing KCH (Frey et al. 2010). The retarded nuclear migration is probably caused by elevated cross-linking of microtubules with the perinuclear actin basket (Klotz and Nick 2012), whereas the stimulated cell elongation is linked with a second subpopulation of KCH kinesins associated with cortical microtubules and uncoupled from actin (Klotz and Nick 2012; Kühn et al. 2013), which preferentially binds to tyrosinated (dynamic) microtubules (Schneider et al. 2015). Although the effect of KCH overexpression resembles that of the Lifeact-psRFP marker with respect to the retarded nuclear movement, the two overexpression lines clearly differ with respect to axis manifestation (promoted for the KCH line, impaired for the Lifeact-psRFP line), and the incidence of tripolar cells (observed only in the Lifeact-psRFP, but not in the KCH lines).

Since KCH binds to microtubules, the principal role of microtubules in polarity and axis formation should be discussed as well at this point. To control cell axis, cortical microtubules must be ordered into parallel arrays, accompanied by cell elongation in a direction perpendicular to microtubule orientation and a progressive alignment of cellulose texture with microtubules. In expanding cylinders, mechanic tension is anisotropic (with transverse doubled over longitudinal tension), such that cylindrical plant cells are expected to widen rather than to elongate (Preston 1955). By transverse deposition of cellulose microfibrils, plant cells can override this mechanic anisotropy and reinforce elongation growth (Green 1980). The previous publication of Zaban et al. (2013) has shown that the stabilization of microtubules via

overexpression of AtTuB6 led to a faster polarity induction and axis formation. It could be shown that, due to overexpression of AtTuB6, microtubules were stabilized, and axis formation was promoted, which requires more efficient alignment of microtubule arrays. A similar promotion of microtubule alignment after treatment had been reported earlier after treatment with taxol (Kuss-Wymer and Cyr 1992). Thus, alignment of cortical microtubules can proceed efficiently with stable microtubules, indicative of a mechanism that is based on mutual sliding. Also for auxin-dependent microtubule reorientation, initial direction-dependent disassembly and reassembly is followed by a second phase, where microtubules coalign and harbor mainly detyrosinated α -tubulin, a marker for microtubule stability (Wiesler et al. 2002). To address the role of microtubule dynamics in our system, we induced destabilization of microtubules via Oryzalin treatment, which eliminates microtubules due to their turnover, which was followed by a delay in polarity induction and axis formation. Furthermore, we could show that Oryzalin-treated protoplasts were not able to elongate (see Figure S4). Thus, microtubules and microtubule dynamics are necessary for axis formation.

Axial cell expansion is delayed in H2B-mEos (see Figure 4), which means that nuclear architecture conveys a signal to axis elongation. Notably, also walled cells of H2B-mEos are significantly shorter compared to the non-transformed cell line (data not shown). It is conceivable that the signal from the interior of the nucleus acts on cytoskeletal targets at the periphery. Also for animal cells a functional relationship between lamins and histones has been reported (Taniura et al. 1995). Since the plant nucleus harbors deep grooves, invaginations and even perforations that are maintained by actin (Collings et al. 2000), changes of intranuclear architecture are expected to alter the organization of the cytoskeleton.

Overexpression of both the perinuclear actin marker Lifeact-psRFP as well as the kinesin GFP-NtKCH, promoted the re-establishment of the cell wall. Thus, although the nuclear positioning itself seems to be dispensable for polarity induction, factors which influence nuclear migration might also influence polarity formation. Our model assumes that retrograde signals are required for polarity induction, which are transduced (transported) through the cytoskeleton to the periphery of the cell and act on cytoskeletal targets at the plasma membrane. Interestingly, also the overexpression of the histone marker H2B-mEos leads to faster formation of the cell wall, indicating that intranuclear architecture modulates the retrograde signaling from the nucleus to the plasma membrane. The nature of this retrograde signal remains to be elucidated. It might be a molecule transported along the cytoskeleton, for instance by interference with vesicle flow by the actin basket, which means chemical signaling. Alternatively, it might be a mechanical signal conveyed by cytoskeletal tensegrity, comparable to recent findings in animal cells, where the perinuclear region was found to be affected due to mechanical stimulation at the cell periphery (Shao et al. 2015). Future work will be dedicated to resolve this question of the two models. To strengthen the model of mechanical/tensegral signaling, cytoskeletal tensegrity can be modulated locally or inducibly and forces transmitted between perinuclear rim and cell periphery can be applied.

To study chemical signaling (for instance via aggregating vesicles), the transport of the retrograde signal can be investigated further as an alternative model.

MATERIALS AND METHODS

Cell lines and cultivation

BY-2 (*Nicotiana tabacum* L. cv Bright Yellow-2) suspension cell lines (Nagata et al. 1992) were cultivated in liquid medium containing 4.3 g/L Murashige and Skoog (MS) salts (Duchefa Biochemie, The Netherlands), 30 g/L sucrose, 200 mg/L KH_2PO_4 , 100 mg/L (myo)-inositol, 1 mg/L thiamine and 0.2 mg/L 2,4-D, pH 5.8. Cells were subcultivated weekly, inoculating 1.0–1.5 mL of stationary cells into fresh medium (30 mL) in 100 mL Erlenmeyer flasks. The cell suspensions were incubated in darkness at 26 °C under constant shaking on a KS260 basic orbital shaker (IKA Labortechnik, Germany) at 150 rpm. In addition to the non-transformed BY-2 wild-type (WT), transgenic lines were used in this study that expressed the actin binding protein Lifeact in fusion with a photo-switchable red fluorescent protein (Lifeact-psRFP, Durst et al. 2014), a kinesin with a calponin homology domain in fusion with GFP isolated either from *Nicotiana tabacum* or from *Oryza sativa* (GFP-NtKCH and GFP-OsKCH, Frey et al. 2009; Klotz and Nick 2012), and a histone marker fused to a photoconvertible protein (H2B-mEos, Wozny et al. 2012), all under the control of a constitutive Cauliflower mosaic virus (CaMV) 35S promoter. Additionally, a free GFP line was used as a control (Nocarova and Fischer 2009; kind gift of J. Petrášek, Charles University, Prague, Czech Republic). The media for the transgenic cell lines were complemented either with 30 mg/L hygromycin (H2B-mEos), with 40 mg/L hygromycin (Lifeact-psRFP), with 25 mg/L kanamycin (free GFP), or with 50 mg/L kanamycin (GFP-NtKCH, GFP-OsKCH), respectively. All experiments were performed using cells after 3 d of subcultivation.

Generation and regeneration of protoplasts

The protocol was adapted from Kuss-Wymer and Cyr (1992) and Zaban et al. (2013) with minor modifications. Aliquots of 4 mL were harvested under sterile conditions 3 d after subcultivation and digested for 1 h at 26 °C in 4 mL enzyme solution of 1% (w/v) cellulase YC (Yakuruto, Tokyo) and 0.1% (w/v) pectolyase Y-23 (Yakuruto, Tokyo) in 0.4 mol/L mannitol at pH 5.5 under constant shaking on a KS260 basic orbital shaker (IKA Labortechnik) at 100 rpm in Petri dishes of 90 mm diameter. After digestion, protoplasts were collected by 500 rpm for 5 min in fresh reaction tubes. The protoplast sediment was carefully resuspended in 10 mL of FMS wash medium (4.3 g/L MS-salts, 100 mg/L (myo)-inositol, 0.5 mg/L nicotinic acid, 0.5 mg/L pyroxidone-HCl, 0.1 mg/L thiamine and 10 g/L sucrose in 0.25 mol/L mannitol (Kuss-Wymer and Cyr 1992; Wymer et al. 1996)). After three washing steps, protoplasts were transferred into 4 mL FMS-store medium (FMS wash medium complemented with 0.1 mg/L 1-naphthaleneacetic acid (NAA), and 1 mg/L benzylaminopurine). Protoplasts were incubated in the dark at 26 °C without shaking in Petri dishes (5 cm diameter). To prevent evaporation, the Petri dishes were sealed with Parafilm[®] M (Bemis Company Inc., Neehna WI, USA). In one

experiment, the FMS-store medium was complemented with 500 nmol/L Oryzalin to eliminate microtubules.

Microscopy and quantifications

To analyze temporal patterns of regeneration for different transgenic BY-2 lines (Lifeact-psRFP, GFP-NtKCH and H2B-mEos) in comparison to non-transformed BY-2 cells, 15 μL of the respective protoplast suspension were carefully mounted on slides using imaging spacers made from silicone (Secure-Seal, Sigma-Aldrich, Neu-Ulm, Germany) to safeguard the protoplast from bursting. For detection, the regenerated cellulosic cell wall was stained by Calcofluor White (1 volume of 0.1% w/v) according to Maeda and Ishida (1967) and Nagata and Takebe (1970). Regeneration was followed over 1 week under an AxioImager Z.1 microscope (Zeiss, Jena, Germany) equipped with an ApoTome microscope slider for optical sectioning and a cooled digital charge-coupled device camera (AxioCam MRm) recording the cells through differential interference illumination by a 20 \times /0.75 plan-apochromat objective and the Calcofluor White signal through the filter set 49 (excitation at 365 nm, beam splitter at 395 nm and emission at 445 nm).

Images were processed and analyzed using the AxioVision software (Rel. 4.8.2) (Zeiss, Jena, Germany). To ensure unbiased acquisition of images, the MosaicX-module sampling system (Zeiss, Jena, Germany) was employed automatically recording individual cells and assembling a large panel of cells covering an area of 5 \times 5 mm consisting of 266 individual images. Individual stages as defined in Figure 1 were scored from those composite images. Stages were defined as follows: stage 1 round, no cell wall; stage 2 cell wall present upon staining with Calcofluor White; stage 3 ovoid shape; stage 4 elongate with a ratio of longer axis to shorter axis of >2.0; stage 5 tripolar shape. Frequency distributions were calculated from 3,000 individual cells per time point from three independent biological replications; error bars represent standard errors of the mean (SE), significance of indicated differences was tested by a paired, two-side t-test.

To follow the regeneration of individual cells, 45 μL of the protoplast suspension were filled into Lab-Tek[™] chambers (Nunc GmbH & Co. KG Thermo Fischer Scientific, Langensfeld, Germany). The suspension was then embedded in 400 μL liquefied FMS-store medium complemented with 0.1% agarose (Sigma-Aldrich Chemie GmbH, Steinheim, Germany) to avoid cells drifting out of focus during recording. Subsequently, the chambers were wrapped with Parafilm[®] M (Bemis Company, Inc., Neehna WI, USA) to maintain humidity, followed by a short centrifugation step with 500 rpm for 1 min (Concentrator 5301, Eppendorf, Hamburg, Germany). Nuclear movement and regeneration of the protoplasts were observed using an AxioObserver Z1 microscope (Zeiss, Jena, Germany). A selected position was defined in x, y and z-axis with the AxioVision software (Rel. 4.8.2, Zeiss, Jena, Germany), and every 3 min an image was recorded automatically with a 20 \times /0.8 Plan-Apochromate objective and differential interference contrast illumination. To generate movies, single frames were compiled into one avi-video by using Image J (National Institutes of Health, Bethesda, MD, USA). For each cell line, 10–20 individual cells were recorded from two or three independent biological replications.

ACKNOWLEDGEMENTS

We thank N. Wunsch and S. Purper for technical assistance. The H2B-mEos was kindly provided by Jaideep Mathur. This work was supported by a Ph.D. fellowship of State of Baden-Württemberg (Landesgraduiertenförderung) to L. Brochhausen and funds from the Deutsche Forschungsgemeinschaft (NI 324/19-1).

AUTHOR CONTRIBUTIONS

L.B. performed the experiments and drafted the manuscript. J.M. and P.N. designed the experiment, supervised the study and revised the manuscript.

REFERENCES

- Ahmad K, Henikoff S (2002) Histone H3 variants specify modes of chromatin assembly. **Proc Natl Acad Sci USA** 99: 16477–16484
- Bartova E, Krejci J, Harnicarova A, Galiova G, Kozubek S (2008) Histone modifications and nuclear architecture: A review. **J Histochem Cytochem** 56: 711–721
- Collings DA, Carter CN, Rink JC, Scott AC, Wyatt SE, Allen NS (2000) Plant nuclei can contain extensive grooves and invaginations. **Plant Cell** 12: 2425–2440
- Deal RB, Henikoff S (2011) Histone variants and modifications in plant gene regulation. **Curr Opin Plant Biol** 14: 116–122
- Durst S, Hedde PN, Brochhausen L, Nick P, Nienhaus GU, Maisch J (2014) Organization of perinuclear actin in live tobacco cells observed by PALM with optical sectioning. **J Plant Physiol** 171: 97–108
- Fransz PF, de Jong JH (2002) Chromatin dynamics in plants. **Curr Opin Plant Biol** 5: 560–567
- Frey N, Klotz J, Nick P (2009) Dynamic bridges - a calponin-domain kinesin from rice links actin filaments and microtubules in both cycling and non-cycling cells. **Plant Cell Physiol** 50: 1493–1506
- Frey N, Klotz J, Nick P (2010) A kinesin with calponin-homology domain is involved in premitotic nuclear migration. **J Exp Bot** 61: 3423–3437
- Fuchs J. (2011) *Characterization and Application of Photoswitchable Fluorescent Proteins for Nanoscopy*. PhD thesis, Karlsruhe Institute of Technology, Karlsruhe, Germany
- Goldman RD, Gruenbaum Y, Moir RD, Shumaker DK, Spann TP (2002) Nuclear lamins: Building blocks of nuclear architecture. **Genes Dev** 16: 533–547
- Goodner B, Quatrano RS (1993) Fucus embryogenesis: A model to study the establishment of polarity. **Plant Cell** 5: 1471–1481
- Green PB (1980) Organogenesis – A biophysical view. **Ann Rev Plant Physiol** 31: 51–82
- Griffis AH, Groves NR, Zhou X, Meier I (2014) Nuclei in motion: Movement and positioning of plant nuclei in development, signaling, symbiosis, and disease. **Front Plant Sci** 5:129
- Hable WE, Hart PE (2010) Signaling mechanisms in the establishment of plant and fucoid algal polarity. **Mol Reprod Dev** 77: 751–758
- Katsuta J, Shibaoka H (1988) The Roles of the cytoskeleton and the cell-wall in nuclear positioning in tobacco BY-2 cells. **Plant Cell Physiol** 29: 403–413
- Klotz J, Nick P (2012) A novel actin-microtubule cross-linking kinesin, NtKCH, functions in cell expansion and division. **New Phytol** 193: 576–589
- Kouzarides T (2007) Chromatin modifications and their function. **Cell** 128: 693–705
- Kühn S, Liu Q, Eing C, Wüstner R, Nick P (2013) Nanosecond electric pulses target to a plant-specific kinesin at the plasma membrane. **J Membr Biol** 246: 927–938
- Kuss-Wymer CL, Cyr RJ (1992) Tobacco protoplasts differentiate into elongate cells without net microtubule depolymerization. **Protoplasma** 168: 64–72
- Lee KK, Starr D, Cohen M, Liu J, Han M, Wilson KL, Gruenbaum Y (2002) Lamin-dependent localization of UNC-84, a protein required for nuclear migration in *Caenorhabditis elegans*. **Mol Biol Cell** 13: 892–901
- Maeda H, Ishida N (1967) Specificity of binding of hexopyranosyl polysaccharides with fluorescent brightener. **J Biochem** 62: 276–278
- Malone CJ, Fixsen WD, Horvitz HR, Han M (1999) UNC-84 localizes to the nuclear envelope and is required for nuclear migration and anchoring during *C. elegans* development. **Development** 126: 3171–3181
- Morris NR (2000) Nuclear migration: From fungi to the mammalian brain. **J Cell Biol** 148: 1097–1101
- Morris NR (2003) Nuclear positioning: The means is at the ends. **Curr Opin Cell Biol** 15: 54–59
- Nagata T, Nemoto Y, Hasezawa S (1992) Tobacco BY-2 cell line as the “HeLa” cell in the cell biology of higher plants. **Int Rev Cytol** 132: 1–30
- Nagata T, Takebe I (1970) Cell wall regeneration and cell division in isolated tobacco mesophyll protoplasts. **Planta** 92: 301–308
- Nick P (2008) Control of cell axis. In: Nick P, ed. *Plant Cell Monographs*. Springer-Verlag, Berlin-Heidelberg. pp. 3–46
- Nick P (2011) Mechanics of the cytoskeleton. In: Wojtaszek P, ed. *Mechanical Integration of Plant Cells and Plants*. Springer-Verlag, Berlin-Heidelberg. pp. 53–90
- Nick P, Furuya M (1992) Induction and fixation of polarity – Early steps in plant morphogenesis. **Dev Growth Differ** 34: 115–125
- Nocarova E, Fischer L (2009) Cloning of transgenic tobacco BY-2 cells; an efficient method to analyse and reduce high natural heterogeneity of transgene expression. **BMC Plant Biol** 9: 44
- Preston RD (1955) Mechanical properties of the plant cell wall. In: Ruhland W, ed. *Handbuch der Pflanzenphysiologie vol. 1*. Springer-Verlag, Berlin-Göttingen-Heidelberg. pp. 745–751
- Schneider N, Ludwig H, Nick P (2015) Suppression of tubulin detyrosination by parthenolide recruits the plant-specific kinesin KCH to cortical microtubules. **J Exp Bot** 66: 2001–2011
- Schneider R, Persson S (2015) Connecting two arrays: The emerging role of actin-microtubule cross-linking motor proteins. **Front Plant Sci** 6:415
- Shao X, Li Q, Mogilner A, Bershadsky AD, Shivashankar GV (2015) Mechanical stimulation induces formin-dependent assembly of a perinuclear actin rim. **Proc Natl Acad Sci USA** 112: 2595–2601
- Smith CM, Haimberger ZW, Johnson CO, Wolf AJ, Gafken PR, Zhang ZL, Parthun MR, Gottschling DE (2002) Heritable chromatin structure: Mapping “memory” in histones H3 and H4. **Proc Natl Acad Sci USA** 99: 16454–16461
- Smith LG (2001) Plant cell division: Building walls in the right places. **Nat Rev Mol Cell Biol** 2: 33–39
- Talbert PB, Masuelli R, Tyagi AP, Comai L, Henikoff S (2002) Centromeric localization and adaptive evolution of an *Arabidopsis* histone H3 variant. **Plant Cell** 14: 1053–1066

- Taniura H, Glass C, Gerace L (1995) A chromatin binding site in the tail domain of nuclear lamins that interacts with core histones. *J Cell Biol* 131: 33–44
- Verbsky ML, Richards EJ (2001) Chromatin remodeling in plants. *Curr Opin Plant Biol* 4: 494–500
- Vöchting H (1878) *Über Organbildung im Pflanzenreich*. Cohen, Bonn
- Wang QY, Nick P (1998) The auxin response of actin is altered in the rice mutant Yin-Yang. *Protoplasma* 204: 22–33
- Wiesler B, Wang QY, Nick P (2002) The stability of cortical microtubules depends on their orientation. *Plant J* 32: 1023–1032
- Wozny M, Schattat MH, Mathur N, Barton K, Mathur J (2012) Color recovery after photoconversion of H2B::mEosFP allows detection of increased nuclear DNA content in developing plant cells. *Plant Physiol* 158: 95–106
- Wymer CL, Wymer SA, Cosgrove DJ, Cyr RJ (1996) Plant cell growth responds to external forces and the response requires intact microtubules. *Plant Physiol* 110: 425–430
- Yi H, Sardesai N, Fujinuma T, Chan CW, Veena, Gelvin SB (2006) Constitutive expression exposes functional redundancy between the *Arabidopsis* histone H2A gene *HTA1* and other H2A gene family members. *Plant Cell* 18: 1575–1589
- Zaban B, Maisch J, Nick P (2013) Dynamic actin controls polarity induction de novo in protoplasts. *J Integr Plant Biol* 55: 142–159

SUPPORTING INFORMATION

Additional supporting information may be found in the online version of this article at the publisher's web-site.

Figure S1. Frequency distribution of cell division in BY-2 Lifeact-psRFP

Frequency distribution of cell division 2 d after protoplast preparation in BY-2 Lifeact-psRFP protoplasts (grey bars) compared to non-transformed BY-2 protoplasts (white bars). Frequency distributions have been calculated from 2 000 individual cells. Error bars show standard errors of the mean (SE). Asterisks represent significance of indicated differences as tested by a paired, two-side t-test (* $P < 5\%$, ** $P < 1\%$).

Figure S2. Frequency distributions of regeneration stages in BY-2 free GFP

Frequency distributions of the different regeneration stages for different time points after protoplast preparation in BY-2 free GFP (light grey bars) compared to non-transformed BY-2 protoplasts (white bars). Stages are indicated schematically. Frequency distributions were calculated from 3 000 individual cells per time point from three independent biological replications. Error bars show standard errors of the mean (SE). Asterisks represent significance of indicated differences as tested by a paired, two-side t-test (* $P < 5\%$, ** $P < 1\%$).

Figure S3. Frequency distributions of regeneration stages in BY-2 GFP-OsKCH

Frequency distributions of the different regeneration stages for different time points after protoplast preparation in BY-2 GFP-OsKCH (black bars) compared to non-transformed BY-2 protoplasts (white bars). Stages are indicated schematically. Frequency distributions were calculated from 3 000 individual cells per time point from three independent biological replications. Error bars show standard errors of the mean (SE). Asterisks represent significance of indicated differences as tested by a paired, two-side t-test (* $P < 5\%$, ** $P < 1\%$).

Figure S4. Frequency distributions of regeneration stages after Oryzalin treatment

Frequency distributions of the different regeneration stages for different time points after protoplast preparation and Oryzalin treatment (500 nmol/L) (light grey bars) compared to non-treated BY-2 protoplasts (white bars). Stages are indicated schematically. Frequency distributions were calculated from 3 000 individual cells per time point from three independent biological replications. Error bars show standard errors of the mean (SE). Asterisks represent significance of indicated differences as tested by a paired, two-side t-test (* $P < 5\%$, ** $P < 1\%$).

Figure S5. Images from BY-2 cells at the peak of proliferation Representative images from BY-2 cells 3 d after subcultivation (A–G). Nuclei are in the cell center. Scale bars = 20 μm .

Movie S1. Time-lapse movie of regenerating non-transformed BY-2 protoplast

Time-lapse movie showing the regeneration of a representative non-transformed BY-2 protoplast followed from d 0 (0 hours after generation of protoplasts) until d 1 (24 h after generation of protoplasts) recording one frame every 3 min. Scale bar = 20 μm .

Movie S2. Time-lapse movie of regenerating BY-2 Lifeact-psRFP protoplasts

Time-lapse movie showing the regeneration of a representative BY-2 Lifeact-psRFP protoplast followed from d 0 (0 hours after generation of protoplasts) until d 1 (24 h after generation of protoplasts) recording one frame every 3 min. Scale bar = 20 μm .

Movie S3. Time-lapse movie of regenerating BY-2 GFP-NtKCH protoplast

Time-lapse movie showing the regeneration of a representative BY-2 GFP-NtKCH protoplast followed from d 0 (0 hours after generation of protoplasts) until d 1 (24 h after generation of protoplasts) recording one frame every 3 min. Scale bar = 20 μm .

Movie S4. Time-lapse movie of regenerating BY-2 H2B-mEos protoplast

Time-lapse movie showing the regeneration of a representative BY-2 H2B-mEos protoplast followed from d 0 (0 hours after generation of protoplasts) until d 1 (24 h after generation of protoplasts) recording one frame every 3 min. Scale bar = 20 μm .